Effect of initial conditions on the mean energy dissipation rate and the scaling exponent

R. A. Antonia[1] and B. R. Pearson[2]
[1]Department of Mechanical Engineering, University of Newcastle, New South Wales 2308, Australia
[2]Fluid Dynamics Laboratory, Department of Applied Physics, Technical University, Eindhoven, The Netherlands
(Received 7 August 2000)

Implications of the expectation that the mean energy dissipation rate $\langle\epsilon\rangle$ should become independent of viscosity at sufficiently large values of R_λ, the Taylor microscale Reynolds number, are examined within the framework of small-scale intermittency and an adequate description of the second-order velocity structure function over the dissipative and inertial ranges. For nominally the same flow, a two-dimensional wake, but with different initial conditions, values of $C_\epsilon \equiv \langle\epsilon\rangle L/u'^3$, the scaling exponent and the Kolmogorov constant differ at the same R_λ.

PACS number(s): 47.27.Vf

I. INTRODUCTION

A basic tenet of turbulence is that the mean energy dissipation rate $\langle\epsilon\rangle$ becomes independent of ν, the kinematic viscosity of the fluid, when the Reynolds number is sufficiently large, e.g., [1–5]. Dimensional arguments, e.g., [1], indicate that

$$\langle\epsilon\rangle = C_\epsilon \frac{u'^3}{L_u}, \tag{1}$$

where the integral turbulence length scale L_u and u' ($\equiv\langle u^2\rangle^{1/2}$, the rms longitudinal velocity fluctuation), characterize the large-scale structure of turbulence. The possible dependence of C_ϵ both with respect to the Reynolds number, flow type, and different initial conditions in a given flow, has attracted a fair amount of attention. Saffman [2] pointed out that the possibility that C_ϵ can depend weakly on the Reynolds number could not be completely dismissed. The detailed examination of decaying grid turbulence by Sreenivasan [3] indicated that the magnitude of C_ϵ decreased with $R_\lambda \equiv u'\lambda/\nu$ (λ is the longitudinal Taylor microscale) becoming approximately constant ($\simeq 1$) at $R_\lambda \simeq 100$. Sreenivasan [3] also noted that the asymptotic value of C_ϵ depends on the particular flow. More recently [5], he suggested, on the basis of direct numerical simulations of homogeneous turbulence in a periodic box that the magnitude of C_ϵ may also depend on the details of forcing at low wave numbers or perhaps the structure of the large scale itself.

The previous considerations have a bearing on a number of issues that are important for turbulence research. For example, C_ϵ appears explicitly in the relations between the integral scale L_u and either λ or the Kolmogorov microscale $\eta = \nu^{3/4}/\langle\epsilon\rangle^{1/4}$. For isotropic turbulence,

$$\frac{L_u}{\lambda} = C_\epsilon \frac{R_\lambda}{15} \tag{2a}$$

and

$$\frac{L_u}{\eta} = C_\epsilon \frac{R_\lambda^{3/2}}{15^{3/4}}. \tag{2b}$$

Consistently, C_ϵ appears in expressions that allow R_λ to be estimated from a characteristic (and simply inferred) Reynolds number Re. For a cylinder wake, $\mathrm{Re} \equiv U_1 d/\nu$, where U_1 is the free stream velocity and d is the cylinder diameter. For a jet, the definition of Re would be based on the jet velocity and either the nozzle width or nozzle diameter. Relations between R_λ and Re were given in [6] for plane and circular jets.

Another issue, considered by Grossmann [7] and Stolovitzky and Sreenivasan [8], is whether the asymptotic constancy of C_ϵ is consistent with the existence of intermittency in the inertial range. These authors used as starting point the K62 [9] relation

$$\langle(\delta u)^2\rangle = C_u (L_u\langle\epsilon\rangle)^{2/3}\left(\frac{r}{L_u}\right)^{\zeta_u}, \tag{3}$$

where C_u is a constant (strictly the K62 constant, which, like the no-intermittency K41 [10] constant, may depend on the macrostructure of the flow). They also assumed that $\langle(\delta_u)^2\rangle$ could be represented, for values of the separation r extending from η through the viscous dissipative range (DR) and into the inertial range (IR), by the interpolation relation [7,8,10–13]

$$\langle(\delta u)^2\rangle = \frac{\langle\epsilon\rangle\eta^2}{15\nu} \frac{(r/\eta)^2}{\left[1+\left(\frac{r}{r_c}\right)^2\right]^{(2-\zeta_u)/2}}, \tag{4}$$

where r_c is the separation corresponding to the crossover between the DR and the IR. Matching the asymptotic form of Eq. (4), when $r \gg r_c$, with Eq. (3) leads to

$$C_u = 15^{-[(1/2)+(3/4)\zeta_u]} r_c^{*\,2-\zeta_u} C_\epsilon^{\zeta_u - 2/3} R_\lambda^{(3/2)\zeta_u - 1}, \tag{5}$$

where, in general, the asterisk denotes normalization by η and/or the Kolmogorov velocity scale $u_K \equiv \nu^{1/4}\langle\epsilon\rangle^{1/4}$. Grossmann [7] concluded that the independence of C_ϵ on R_λ was an argument against IR scaling corrections if one dismisses the possibility that r_c^* can vary with R_λ, viz.,

$$r_c^* \sim R_\lambda^{[1-(3/2)\zeta_u]/(2-\zeta_u)}, \tag{6}$$

so that C_u remains constant. Stolovitzky and Sreenivasan [8] concluded that Eq. (6) is a real possibility having first established, using an independent argument, that C_ϵ is independent of R_λ if and only if C_u is independent of R_λ [13].

The present paper provides new insight into the possible dependence of all the parameters that appear in Eq. (5) on initial conditions and also R_λ. This should permit Eq. (6) to be tested in a relatively general context. Implicit in all of the above discussion is the assumption that ζ_u is also constant, though different from $\frac{2}{3}$, when R_λ is sufficiently large for C_ϵ, and possibly C_u, to be considered constant. The relation between C_ϵ and C_u, viz.,

$$C_\epsilon \simeq \left(\frac{2}{C_u}\right)^{3/2}, \tag{7}$$

which was obtained by [8] after substituting $r=L_u$ in Eq. (3), is somewhat tenuous in the context of the requirement $\eta \ll r \ll L_u$ for the existence of an IR [9,11]. Note that Eq. (7) implies that C_u, like C_ϵ, is likely to depend on the nature of the flow and/or initial conditions; any claim of universality for C_u would not be easily reconcilable with Eq. (7). It should also be pointed out that the argument put forward by [8] to suggest that r_c^* should depend on R_λ does not have strong experimental support. The use of the Kolmogorov equation [14], together with Eq. (4), leads to [8]

$$r_c^{*2} = 12(15)^{1/2}\frac{(\zeta_u - 2)}{S_{\partial u/\partial x}}, \tag{8}$$

where $S_{\partial u/\partial x} \equiv \langle(\partial u/\partial x)^3\rangle / \langle(\partial u/\partial x)^2\rangle^{3/2}$ is the skewness of $\partial u/\partial x$. The available data (e.g., [15]) indicate a relatively broad range of R_λ over which S is approximately constant. The constancy of r_c^* would either violate intermittency (i.e., $\zeta_u = \frac{2}{3}$) or allow for a possible R_λ dependence of C_ϵ, viz.,

$$C_\epsilon \sim R_\lambda^{[1-(3/2)\zeta_u]/(\zeta_u - 2/3)}. \tag{9}$$

If $\zeta_u \simeq 0.7$, then $C_\epsilon \sim R_\lambda^{-3/2}$, i.e., quite a strong (and unlikely) R_λ dependence. Alternatively, if both r^* and C_ϵ are R_λ-independent, and relation (7) is ignored, relation (5) would indicate that

$$C_u \sim R_\lambda^{(3/2)\zeta_u - 1}. \tag{10}$$

For $\zeta_u \simeq 0.7$, $C_u \sim R_\lambda^{0.05}$, a realistic possibility in view of the experimental uncertainty associated with the estimation of C_u. The high R_λ data considered by Praskovsky and Oncley [16] indicate that C_u decreases as $R_\lambda^{-0.1}$; for these data, C_ϵ varied considerably from about 0.5 for the two laboratory experiments to values in the range 1 to 3 for the atmospheric surface layer experiments. Such a variability would contravene the conditions which underpin Eq. (10).

In Sec. III, the magnitude of C_ϵ is obtained, for approximately the same R_λ range, in nominally the same flow, a two-dimensional wake, though with significantly different initial conditions. In one case, the wake is generated by a circular cylinder, while in the other, a flat plate, placed normal to the flow, is used. For these two flows, we also consider (Sec. IV) the R_λ dependencies of ζ_u, r_c^*, and C_u.

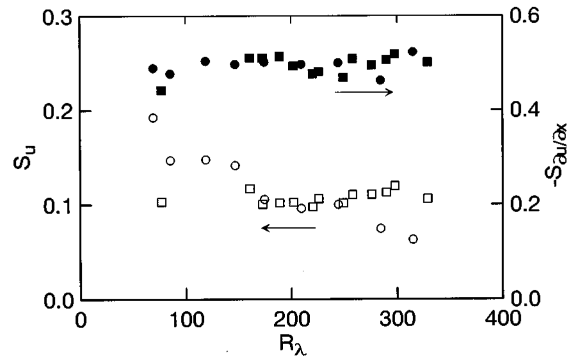

FIG. 1. Dependence of the skewnesses of u (S_u) and $\partial u/\partial x$ ($S_{\partial u/\partial x}$) on R_λ. ○, circular cylinder; □, normal plate; open symbols, S_u; solid symbols, $S_{\partial u/\partial x}$.

II. EXPERIMENTAL DETAILS

The circular cylinder or flat plate is placed at $x=200$ mm downstream of the contraction and spans the width of the working section ($350\times 350\ \mathrm{mm}^2 \times 2.5$ m long) of a blowdown-type open circuit wind tunnel (see [17] for further details). The smooth aluminum circular cylinder diameter d is 28.25 mm and measurements are acquired at $x/d \sim 54$. At this station, $u'/\langle U\rangle$ is $\sim$6–7.3 % and $u'/\langle U\rangle \sim R_\lambda^{0.05}$. The mild steel normal plate (height d of 25 mm) is 5 mm thick with 45° chamfered edges. Measurements are acquired at $x/d \sim 62$. For this flow, $u'\langle U\rangle$ is $\sim$7.5–7.8 % and is virtually R_λ-independent ($u'/\langle U\rangle \sim R_\lambda^{0.01}$).

In each flow, a single-wire probe, with a wire diameter $d_w = 1.27\ \mu$m (Pt-Rh 10%) and an etched length of $200 d_w$, is used to measure the longitudinal (u) velocity fluctuation on the centerline only. All velocity signals are acquired with in-house designed constant temperature anemometers, amplifiers, and low-pass filters (24 dB/octave). The voltage signal from the anemometer is buck-and-gained and, in all cases, the signal is low-pass filtered at a filter frequency f_c at least below half the sampling frequency f_s.

III. SOME FLOW CHARACTERISTICS AND DIMENSIONLESS CONSTANT C_ϵ

The magnitude of $S_{\partial u/\partial x}$ (Fig. 1) is very similar for the two flows ($\sim$0.5–0.6) whereas S_u differs significantly. For the circular cylinder wake, S_u decreases as $\sim R_\lambda^{-0.26}$, while for the normal plate wake, S_u is only weakly dependent ($\sim R_\lambda^{0.03}$) on R_λ. The magnitude of S_u for the two wakes is comparable for the R_λ range considered. The different large-scale behaviors is attributed to the fact that the separation point of the flow from either side of the circular cylinder is R_λ-dependent—i.e., directly dependent on the condition of the boundary layer which separates from the cylinder surface—whereas for the normal plate, the flow always separates from a sharp chamfered edge, an R_λ-independent behavior. The R_λ independence of S_u for the normal plate suggests that this flow will always exhibit a large-scale anisotropy due to the R_λ-independent generation of the macrostructure at the wake generator. It is plausible that, for the circular cylinder, S_u will tend to zero as $R_\lambda \to \infty$, implying that the macrostructure will approach isotropy. However, the

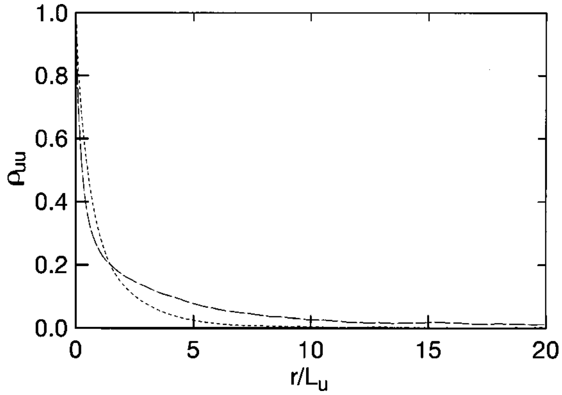

FIG. 2. Longitudinal velocity autocorrelation coefficient. – –, circular cylinder wake $R_\lambda \sim 285$; ---, normal plate wake $R_\lambda \sim 290$.

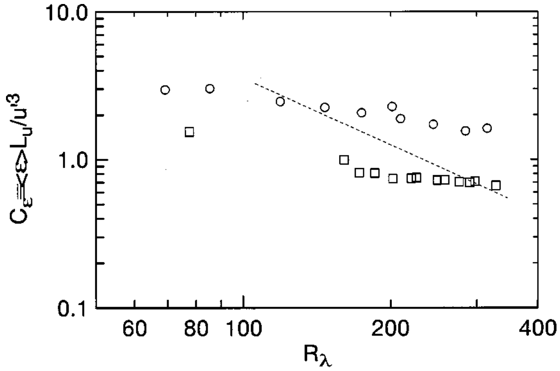

FIG. 3. Variation of $C_\epsilon \equiv \langle \epsilon \rangle L/u'^3$ with R_λ. ○, circular cylinder; □, normal plate. – –, Eq. (9), i.e., $C_\epsilon \sim R_\lambda^{-3/2}$ when $\zeta_u \simeq 0.7$.

magnitude and R_λ dependence of $-S_{\partial u/\partial x}$ are similar in the two flows, suggesting similarity for the smallest scales.

The estimation of C_ϵ requires $\langle \epsilon \rangle$ and L_u to be evaluated. The isotropic value of $\langle \epsilon \rangle$ $[\equiv 15\nu \langle (\partial u/\partial x)^2 \rangle$ with $\langle (\partial u/\partial x)^2 \rangle = \int_0^\infty k_1^2 \phi_u(k_1) dk_1]$ is used for the two flows. The accurate estimation of $\langle \epsilon \rangle$ is dependent on probe resolution and response. All of the current experimental data are corrected spectrally, using a variant of Wyngaard's [18] method, for the attenuation due to the wire length. For the circular cylinder wake, the effective wire sensing length $l_w^* \equiv l_w/\eta$ increases with R_λ (0.47–2.48) while the ratio f_c/f_k decreases from 1.4 to 0.7. Corresponding variations for the normal plate wake are $1.2 \lesssim l_w^* \lesssim 3.0$ and $1.47 \gtrsim f_c/f_k \gtrsim 1.0$. The number $N \equiv \langle U \rangle T_s/2L_u$ (T_s is the total record duration) of independent samples increases with R_λ (6500 and 7500 to 50 000 and 195 000 for the cylinder and normal plate wakes, respectively) and was sufficiently large to ensure convergence of all statistics discussed in this work.

L_u is estimated from the corrected spectrum $\phi_u(k_1)$ via the transformation $\langle u(t)u(t+\tau) \rangle = \int_0^\infty \phi_u(k_1) \cos(k_1 r) dk_1$. A key assumption of this method is that the correlation coefficient $\rho_{uu}(\tau)$ is well-behaved, decaying exponentially to zero as τ increases. Figure 2 shows that $\rho_{uu}(\tau)$ is well-behaved in the plate wake but the approach to zero is quite slow in the circular cylinder wake. Correspondingly, the uncertainty in L_u is larger for this flow ($L_u = 104 \pm 18$ mm) than for the plate wake ($L_u = 46 \pm 1$ mm).

For the two flows, the magnitude of C_ϵ (Fig. 3) decreases with R_λ, the behavior suggesting a relatively slow, asymptotic approach towards a constant at sufficiently large R_λ. As anticipated, the rapid $R_\lambda^{-3/2}$ decay (for $\zeta \simeq 0.7$) implied by relation (9) is not supported by the data. For the circular cylinder wake, the magnitude is nearly twice as large as for the plate wake. This difference reflects to a large extent the larger value of L_u in the cylinder wake (Fig. 2). Sreenivasan also reported the variation of C_ϵ with Re, obtained using particle image velocimetry, on the centerline of a circular cylinder wake at $x/d = 50$. The asymptotic value of C_ϵ ($\simeq 0.6$) is nearly the same as that obtained in the present plate wake. This result may not be too surprising if there are other initial conditions apart from the shape of the wake generator, such as, for example, the free stream turbulence intensity and length scale, which influence the values of $\langle \epsilon \rangle$, L_u, and u'. As noted in the Introduction, the magnitude of C_ϵ determines the precise form of the relationship between R_λ and a global Reynolds number (see Fig. 4). It is relatively easy to show that $R_\lambda = 15^{1/2} C_\epsilon^{-1/2} R_L^{1/2}$, where $R_L \equiv u' L_u/\nu$. From a practical point of view, it is more useful to relate R_λ to Re; the previous expression can be recast as $R_\lambda = 15^{1/2} C_\epsilon^{-1/2} \beta^{1/2} \mathrm{Re}^{1/2}$, where $\beta \equiv (u'/U_0)(U_0/U_1)(L_u/d)$ and U_0 is the local mean velocity defect. For $R_\lambda \gtrsim 200$, the parameter $(\beta/C_\epsilon)^{1/2}$ has about the same magnitude ($\simeq 0.42$) in the two flows so that the resulting expression is $R_\lambda \simeq 1.63\,\mathrm{Re}^{1/2}$ in each case. This expression is closely satisfied by the plate wake data but only approached at the largest values of Re by the cylinder wake data. The previous trend is consistent with our observations that the plate wake reaches self-preservation more rapidly than the cylinder wake.

IV. SCALING EXPONENT AND KOLMOGOROV CONSTANT

The scaling exponent ζ_u, shown in Fig. 5, was estimated by applying relation (4) to the measured (and corrected) distributions of $\langle (\delta u^*)^2 \rangle$. The maximum value $r^*_{\max}$ used in implementing the least-squares fit corresponded to the value of r^* at which the magnitude of $\langle (\delta u^*)^3 \rangle / r^*$ is maximum (a discussion of $r^*_{\max}$ was given in [19]).

The dependence of ζ_u on R_λ (Fig. 5) is similar for the two flows. The magnitude of ζ_u decreases between $R_\lambda \simeq 100$ and 250; it then appears to increase slowly for $R_\lambda > 250$. The maximum value of R_λ is clearly insufficient to ascertain whether ζ_u has become constant. It is clear, however, that,

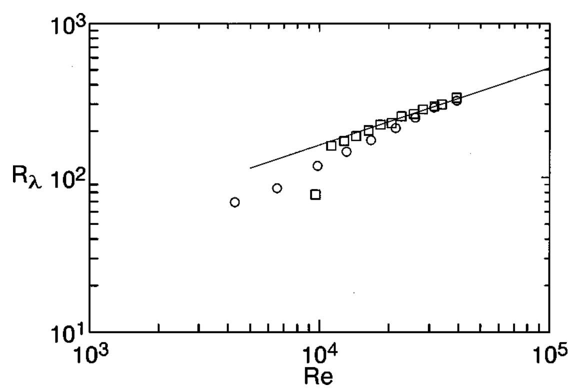

FIG. 4. Relation between R_λ and Re. ○, circular cylinder; □, normal plate. —, $R_\lambda = 1.63 Re^{1/2}$ (described in the text).

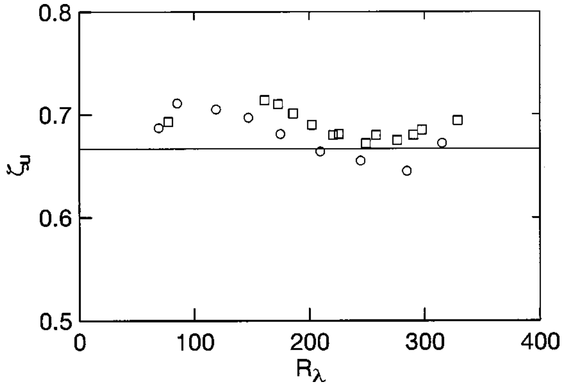

FIG. 5. Scaling exponent ζ_u for the second-order longitudinal structure function $\langle(\delta u^*)^2\rangle$ calculated by Eq. (5). ○, circular cylinder; □, normal plate. The solid line ($\zeta_u=\frac{2}{3}$) corresponds to K41.

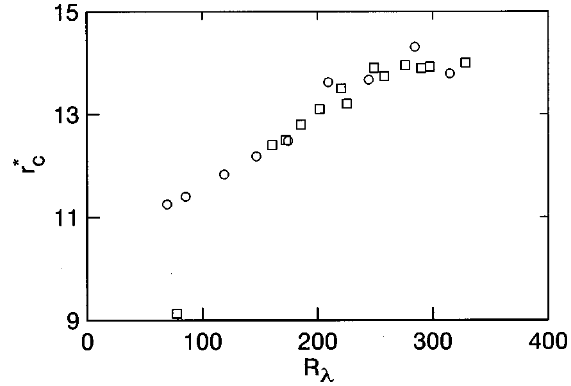

FIG. 7. Scale r_c^* corresponding to crossover between the dissipative range and scaling range. ○, circular cylinder; □, normal plate.

irrespective of R_λ, the magnitude is larger in the plate wake than in the cylinder wake. It seems likely that the asymptotic values, at large R_λ, will also differ in the two flows.

The existence of a true inertial range, which satisfies the K41 requirement, has been queried [20] in the context of atmospheric Reynolds numbers. Consistently, for the present small/moderate values of R_λ, there is no inertial range. Direct checks of local isotropy were not made in the present experiment as only the u-velocity component was measured. Figure 6 shows, however, that the distribution of $\langle(\delta u^*)^2\rangle$, estimated by Fourier-transforming the corrected distribution of $\phi_u(k_1)$, does not exhibit a well-defined power law over a region that might be loosely identified with the scaling range. Specifically, the magnitude of the derivative $d(\log_{10}\langle(\delta u^*)^2\rangle)/d(\log_{10}r^*)$ is not constant in the region $30 \lesssim r^* \lesssim 130$ (or $1.5 \lesssim \log_{10}r^* < 2.1$), where a power-law range may have been expected. Over this range, the rate of decrease of the derivative is small, which suggests that an ''averaged'' value of ζ_u may be reasonable. It is only in this optic that the values of ζ_u in Fig. 5 should be regarded. In particular, the value of ζ_u obtained from Eq. (4) does appear to represent a reasonable average over the region ($1.5 \lesssim \log_{10}r^* \lesssim 2.1$). We have checked that the application of Eq. (4) yields a decrease in ζ_u when $r^*_{\max}$ increases, in qualitative agreement with the trend shown by the derivative in Fig. 6. Note that the derivative asymptotes to 2 at small r^* [this follows from the requirement than $\langle(\delta u^*)^2\rangle \sim r^{*2}$ as $r^* \to 0$] while the approach to zero at large r^* is slower for the plate wake than the cylinder wake (reflecting the inequality in L_u between the two flows). The two distributions of $\langle(\delta u^*)^2\rangle$ (Fig. 6) are virtually identical throughout the dissipative range.

Apart from yielding an ''averaged'' value of ζ_u, Eq. (4) also provides an estimate of r_c^*, which can be identified with the scale at which the crossover between the dissipative and scaling ranges takes place. Figure 7 shows that r_c^* increased with R_λ and appears to become constant ($\simeq 14$) beyond $R_\lambda \simeq 250$. Stolovitzky and Sreenivasan [8] obtained an expression for r_c^* expanding the terms in Kolmogorov's equation in powers of r and matching the coefficients of r^3. When applied to the present data, Eq. (8) yields a value of r_c^* of about 10.4, independently of R_λ (for $R_\lambda \gtrsim 100$); this trend reflects the nearly similar dependencies on R_λ exhibited by ζ_u (Fig. 5) and $-S_{\partial u/\partial x}$ (Fig. 1). The difference between the distributions of r_c^*, obtained from Eq. (4) and Eq. (8), is likely to be due to the requirements of Kolmogorov's equation being violated, given that the present flow is locally nonhomogeneous and anisotropic.

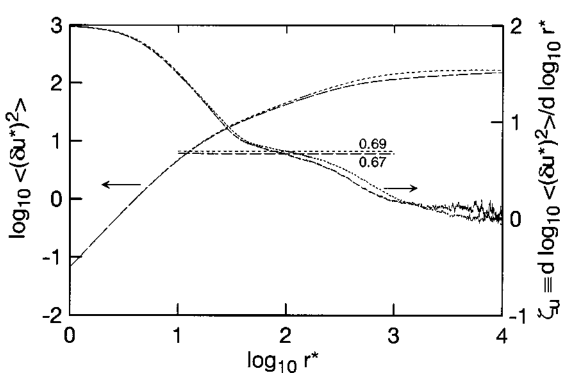

FIG. 6. Variation with respect to $\log_{10}r^*$ of $\log_{10}\langle(\delta u^*)^2\rangle$ and its derivative. $\log_{10}\langle(\delta u^*)^2\rangle$: –––, circular cylinder ($R_\lambda \simeq 315$); ---, normal plate ($R_\lambda \simeq 329$). The horizontal lines represent the values of ζ_u obtained by applying the interpolation relation (4) to the data for $\langle(\delta u^*)^2\rangle$ up to $r^*=r^*_{\max}$, corresponding to the maximum value of $[\langle(\delta u^*)^3\rangle/r^*]$.

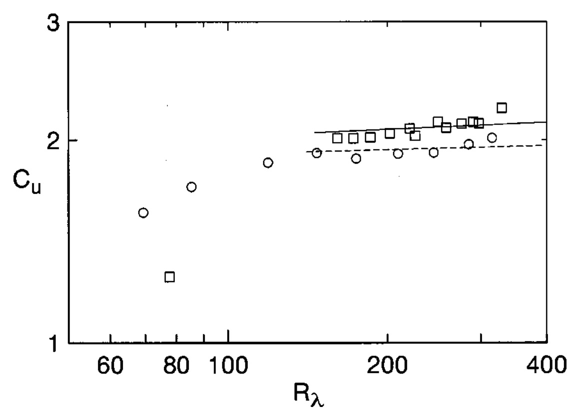

FIG. 8. Kolmogorov constant C_u, calculated using Eq. (5). ○, circular cylinder; □, normal plate. The lines are the rates of increase corresponding to relation (10): —, $C_u \sim R_\lambda^{0.035}$, based on $\zeta_u = 0.69$; — —, $C_u \sim R_\lambda^{0.02}$, based on $\zeta_u = 0.68$.

The magnitude of C_u was estimated from Eq. (5) using the measured values of C_ϵ and the values of ζ_u and r_c^* inferred from Eq. (4). The resulting distributions (Fig. 8) exhibit a rapid increase up to $R_\lambda \simeq 150$ followed by a slow rise. The power-law variations in Fig. 8 are deduced from relation (10) using averaged values of ζ_u ($\simeq 0.68$ and 0.69 for the cylinder and plate wake, respectively). They reflect the experimental trends reasonably well. It is of interest to consider whether there are differences in large-scale anisotropy, as measured, for example, by the ratio v'/u' (v is the transverse velocity fluctuation), between the two flows, which may account for the observed differences in C_u and C_ϵ. Data—obtained in a separate (unpublished) study with a one-component vorticity probe—indicate that v'/u' is about 1.1 for the plate compared to about 0.87 in the cylinder wake. This difference may explain the relative behaviors of C_u (and C_ϵ) in the two flows but a more detailed investigation is needed to establish such a connection more rigorously. The magnitude of C_u is larger for the plate than the cylinder wake. The consensus value ($C_u \simeq 2$), estimated by Yaglom [21] for a wide range of data, lies between the plate wake and cylinder wake values of C_u.

V. CONCLUSIONS

The results of the present experimental investigation clearly indicate that, for nominally the same flow (a two-dimensional wake) and the same R_λ, the magnitude of the dimensionless turbulent mean energy dissipation rate depends on the initial conditions. It is a factor of 2 larger in the cylinder wake than in the plate wake. This dependence on initial conditions corroborates and extends the previous results of Sreenivasan [3–5]. This dependence needs to be taken into account when inferring the value of R_λ, at a given location of the flow, from a knowledge of Re, the global Reynolds number.

The initial conditions also affect the ''averaged'' value of the scaling exponent as well as the magnitude of the Kolmogorov constant. Clearly, these dependencies need to be accounted for when the mean energy dissipation rate is determined using the Kolmogorov (either 1941 or 1962) phenomenology.

ACKNOWLEDGMENT

The support of the Australian Research Council is gratefully acknowledged.

[1] L. D. Landau and E. M. Lifshitz, *Fluid Mechanics* (Pergamon, Oxford, 1986).
[2] P. G. Saffman, in *Topics in Nonlinear Physics*, edited by N. Zabusky (Springer, Berlin, 1968), p. 487.
[3] K. R. Sreenivasan, Phys. Fluids **27**, 1048 (1984).
[4] K. R. Sreenivasan, in *Symposium on Developments in Fluid Dynamics and Aerospace Engineering*, edited by S. M. Deshpande, A. Prabhu, K. R. Sreenivasan, and P. R. Viswanath (Interline, Bangalore, 1995), pp. 159–190.
[5] K. R. Sreenivasan, Phys. Fluids **10**, 528 (1998).
[6] R. A. Antonia, B. R. Satyaprakash, and A. K. M. F. Hussain, Phys. Fluids **23**, 695 (1980).
[7] S. Grossmann, Phys. Rev. E **51**, 6275 (1995).
[8] G. Stolovitzky and K. R. Sreenivasan, Phys. Rev. E **52**, 3242 (1995).
[9] A. N. Kolmogorov, J. Fluid Mech. **13**, 82 (1962).
[10] A. N. Kolmogorov, Dokl. Akad. Nauk SSSR **30**, 299 (1941).
[11] L. Sirovich, L. Smith, and V. Yakhot, Phys. Rev. Lett. **72**, 344 (1994).
[12] C. Meneveau, Phys. Rev. E **54**, 3657 (1996).
[13] G. Stolovitzky, K. R. Sreenivasan, and A. Juneja, Phys. Rev. E **48**, R3217 (1993).
[14] A. N. Kolmogorov, Dokl. Akad. Nauk SSSR **32**, 19 (1941).
[15] K. R. Sreenivasan and R. A. Antonia, Annu. Rev. Fluid Mech. **29**, 435 (1997).
[16] A. A. Praskovsky and S. Oncley, Phys. Rev. Lett. **73**, 3399 (1994).
[17] L. W. B. Browne and R. A. Antonia, Phys. Fluids **29**, 709 (1986).
[18] J. C. Wyngaard, J. Sci. Instrum. **2**, 983 (1968).
[19] R. A. Antonia, B. R. Pearson, and T. Zhou, Phys. Fluid **12**, 3000 (2000); R. A. Antonia, T. Zhou, and G. Xu, Phys. Fluids **12**, 1509 (2000).
[20] K. R. Sreenivasan and B. Dhruva, Prog. Theor. Phys. Suppl. **130**, 103 (1998).
[21] A. M. Yaglom, Izv. Atmos. Ocean. Phys. **17**, 1235 (1981).